electronics

MDPI

Article

Performance Analysis of Vilnius Chaos Oscillator-Based Digital Data Transmission Systems for IoT

Ruslans Babajans *,†, Darja Cirjulina †, Filips Capligins, Deniss Kolosovs, Juris Grizans and Anna Litvinenko

Institute of Radioelectronics, Riga Technical University, Kipsalas St. 6A, LV-1048 Riga, Latvia
* Correspondence: ruslans.babajans@rtu.lv
† These authors contributed equally to this work.

Abstract: The current work is devoted to chaos oscillator employment in digital communication systems for IoT applications. The paper presents a comparative performance analysis of two different chaos data transmission systems: frequency-modulated chaos shift keying (FM-CSK) and quadrature chaos phase-shift keying (QCPSK), and a comparison to their non-chaotic counterparts: frequency-shift keying (FSK) and quadrature amplitude modulation (QAM). For both chaotic communication systems, the Vilnius oscillator and substitution method of chaotic synchronization are chosen due to simple circuitry implementation and low power consumption properties. The performance of the systems in the fading channel with additive white Gaussian noise (AWGN) is evaluated. Also, the systems' performance in the case phase noise is investigated, and the benefits of chaotic waveforms employment for data transmission are demonstrated.

Keywords: nonlinear systems; chaos shift keying; chaos oscillator; chaotic synchronization; communication system; signal processing; chaos shift keying; frequency modulation; wireless sensor networks; internet of things

Citation: Babajans, R.; Cirjulina, D.; Capligins, F.; Kolosovs, D.; Grizans, J.; Litvinenko, A. Performance Analysis of Vilnius Chaos Oscillator-Based Digital Data Transmission Systems for IoT. *Electronics* **2023**, *12*, 709. https://doi.org/10.3390/electronics12030709

Academic Editors: Elena V. Efremova, Alexander S. Dmitriev and Stavros G. Stavrinides

Received: 15 January 2023
Revised: 27 January 2023
Accepted: 29 January 2023
Published: 31 January 2023

1. Introduction

Recent years have shown tremendous growth in wireless sensor networks (WSN) and Internet of things (IoT) devices. Ericson's mobility report [1] states that the number of IoT connections will increase from 13.2 billion to 34.7 billion in the next five years. Such an increase in IoT devices will lead to a significant increase in data volume, necessitating improved security measures. Over the last few years, security research on IoT networks has been focused on Blockchain [2], fog computing [3], and encryption [4]. The major shortcoming of the blockchain in IoT is limited IoT network throughput, while fog computing cannot process requests at heavy loads and sends them to the cloud [3]. The employment of artificial intelligence for traffic management and network structure optimization can reduce this shortcoming of fog computing. Conventional encryption algorithms are not desirable for IoT systems as devices have limited computing and storage resources [5]. The use of physical layer security methods is proposed in [6,7] to address the aforementioned issues. One of the possible solutions for physical layer security enhancement is chaos usage, especially considering that the number of digital communication systems that use chaos phenomena has increased [8] in the last decades. Chaotic signals generally have such properties as very narrow autocorrelation, low cross-correlation, and a noise-like waveform on one hand and high sensitivity to the initial conditions or systems parameter changes and determinism on the other hand. Thus, in combination with coherent modulation techniques, it makes it difficult to detect and interpret the signal without knowing the exact parameters of the system, providing increased security on the physical layer of communication systems [9]. For example, the efficiency and feasibility of the chaotic image cryptosystem have been verified on an experimental platform for secure IoT communication [10]. Moreover, the use of chaotic signals can provide a certain level of resistance to intersymbol interference and channel noise when used in spread spectrum techniques [11].

The properties of chaotic signals provide broad application opportunities in different areas. For example, [12] uses chaotic systems with high entropy for image encryption. In [13], chaotic tags and sensors that exploit the high sensitivity response to changes in chaotic circuit parameters are studied. In radar systems [14], chaotic signals also find practical application due to their wideband nature, thus providing low sensitivity to jamming and interference while being relatively simple to implement and process. Also, chaotic oscillators find their applications in digital communication systems [8], including digital link establishment in WSNs [15]. Some recent studies show a trend in developing new communication systems with an emphasis on improving the security of the transmission channel. The authors of [16] propose using a nine-dimensional modified Lorenz chaos generator in a chaotic masking communication scheme. The increased order chaos generator benefits because of the wider band of a chaotic signal, which is harder to distinguish from noise during transmission. Another approach to improve the secrecy of the communication channel is proposed in [17], where a novel symmetry-based chaotic modulation technique exhibits identical spectral characteristics for different bits transmission, making it more difficult to decode by eavesdroppers.

The chaos signal sources can be divided into two classes—continuous-time and discrete-time systems. The dynamics of continuous-time chaotic systems are described using differential equations. This group mainly consists of analog chaos oscillators. The minimal requirement for the circuit to exhibit chaotic behavior is at least one nonlinear element, one active element, and three energy storage elements [18]. Examples of well-known chaos oscillators are Chua's circuit [18], the Rossler generator [19], and the Lorenz generator [20]. This work considers the Vilnius chaos oscillator [21] as more suitable for application in WSN and IoT due to circuitry simplicity and low energy consumption properties. This group also includes chaotic circuits for which chaos is a side effect of signal switching, as demonstrated in [22–24] for DC-DC converters. The discrete-time systems are described with difference equations and include chaotic maps—nonlinear functions that exhibit chaotic behavior [9]. The most notable examples of chaotic maps include the Logistic map [25], the Henon map [26], and the Gaussian map [27]. Discrete chaotic systems are also implemented by transforming the differential equations of continuous-time chaos oscillators into difference equations [28].

These benefits of chaos use in modern communication systems, including WSN and IoT (such as security aspects enhancement, spread-spectrum, multiple access, etc.), and the variety of available approaches for generating chaotic signals led to the development of various chaos-based modulation schemes. Generally, chaos-based communication systems can be divided into two classes—modulation schemes with coherent and non-coherent detection [29]. Chaotic communication systems with non-coherent detection are based on manipulating chaos signal properties. They are more robust to channel noise than coherent systems but provide less signal protection as information decoding is mainly based on the difference of signals' statistical properties. The modulation schemes of this group are chaos on–off keying (COOK) [30] and differential chaos shift keying (DCSK) [31]. Chaotic communication systems that use coherent detection take advantage of chaotic synchronization—an approach of coupling two chaotic oscillators so that the state variables of the receiver's chaos signal source match those of the transmitter's chaos signal source. To establish chaotic synchronization, at least one of the state variables should be transmitted to the receiver. The reconstruction of the state of the transmitter's chaos signal source in the receiver and transmitted information decoding is possible only if the structure and all parameters of the chaotic oscillator are known, and they are synchronized. Chaotic synchronization improves communication security but decreases resistance to channel noise as a trade-off. The modulation schemes that refer to this group are chaos shift keying (CSK) [32], quadrature chaos shift keying (QCSK) [33], chaos-based code division multiple access (CDMA) [34], and chaotic pulse-position modulation (CPPM) [35].

Due to their wideband nature, narrow autocorrelation function, and low cross-correlation, chaotic signals exhibit relatively good noise immunity and resistance to multipath prop-

agation and multiuser interference, as shown [36–43]. For noise immunity of chaotic communication systems with coherent detection, the performance of the synchronization method is important. For instance, the emphasis on developing an adaptive and noise-robust method of multi-state chaotic synchronization was made in [44] with two non-identical chaos generators (Chen and Chua circuits). In turn, the study [45] analyzes the performance of a novel DCSK chaotic communication system in a Rayleigh channel, concluding that such a system can provide acceptable multipath resistance for up to four simultaneous users.

Regardless of the increasing interest in chaos application in WSN and IoT [46–50] in recent years, there are still many challenges in chaotic communication systems, especially considering noise immunity, multipath propagation resistance, and multiuser interference issues. Therefore, it is crucial to perform research in this area and discover more potential advantages of chaotic communication systems, especially for application in WSN. It should also be noted that, judging by the amount of literature, digital chaotic communication systems based on chaotic maps, as well as non-coherent detection chaotic systems, have been studied much more than coherent detection systems based on continuous-time chaos oscillators [29,36,38,39,41,45,51,52]. This leads to the conclusion that multipath propagation and phase noise impact on the communication systems with chaotic oscillators' employment are insufficiently investigated. Therefore, the present work studies the performance of two novel coherent chaos data transmission systems: frequency-modulated chaos shift keying (FM-CSK) and quadrature chaos phase-shift keying (QCPSK), which are proposed by the authors in [53] and [54], respectively. While the previous works have demonstrated the developed prototypes of the two systems, this one focuses on studying the performance of the FM-CSK and QCPSK in the multipath propagation conditions, additive white Gaussian noise (AWGN) impact, and phase noise's effect on the communication quality. To present a comprehensive analysis, the results for the two systems are compared to their non-chaotic counterparts: frequency-shift keying (FSK) and quadrature amplitude modulation (QAM).

This paper consists of 5 sections. Section 2 explains the concepts and structure of the proposed FM-CSK and QCPSK communication systems and the core element of systems—Vilnius chaos oscillator, as well as the hardware implementation of both communication systems. In Section 3, the results of the multipath propagation study are shown. Section 4 presents the analysis of phase noise's impact on transmission quality. Section 5 concludes the paper.

2. FM-CSK and QCPSK Communication Systems

The current section describes the frequency-modulated chaos shift keying (FM-CSK) and quadrature chaos phase-shift keying (QCPSK) data transmission systems. Both systems presented in the section utilize chaotic waveform as an information carrier to increase the security level of information transfer, yet the systems use similar principles of frequency-shift keying (FSK) and quadrature amplitude modulation (QAM). The section further outlines the main nodes that form the FM-CSK and QCPSK communication systems and the hardware implementation of the two systems, outlining the hardware components used to implement the main nodes of the systems. The section also describes the source of chaotic signals—the Vilnius chaos oscillator and the use of chaotic signals in each system.

2.1. Conceptual Models

Figures 1 and 2 show the block diagrams of the QCPSK and FM-CSK. The transmitter and the receiver of the two systems contain chaos oscillators. The X_1, X_2, and X_3 depict the chaos signals (state variables) of the transmitter's chaos oscillator, while Y_1, Y_2, and Y_3 depict the chaos signals (state variables) of the receiver's chaos oscillator. Both systems are based on coherent chaos signal detection. The chaos oscillators are synchronized using the Pecora–Carrol method [55]. The X_2 signal is transmitted, and the received X'_2 signal substitutes the Y_2 state variable of the receiver's chaos oscillator. As a result, X_1 repeats the behavior of Y_1, and X_3 repeats the behavior of Y_3. The main difference between the

systems is how the binary information signal $b(t)$ and the synchronization signal X_2 are used for modulation and demodulation, as well as how the received information signal $b'(t)$ is detected.

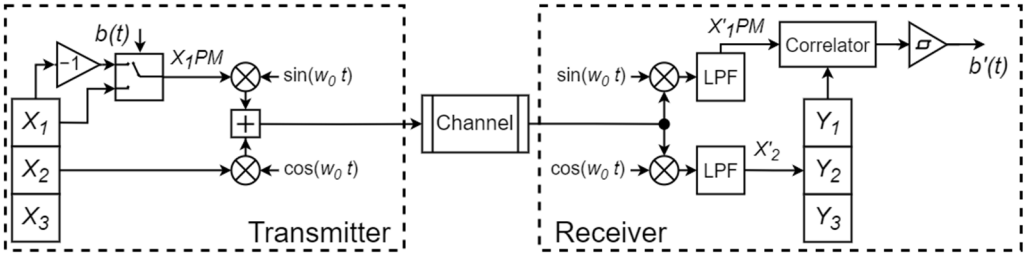

Figure 1. Block diagram of QCPSK data transmission system.

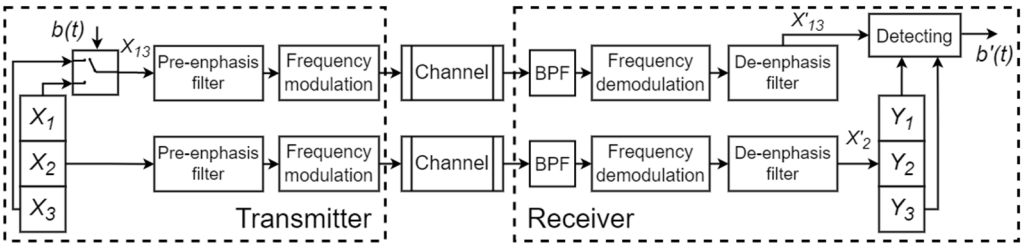

Figure 2. Block diagram of FM-CSK data transmission system.

The QCPSK data transmission system in Figure 1 is based on chaos phase-shift keying and quadrature transceiver. The binary message signal $b(t)$ controls a switch that toggles between X_1 and $-X_1$. Bit "1" shifts to X_1, and bit "0" shifts to $-X_1$, thus forming the phase-manipulated chaos signal labeled as X_1PM. The synchronization X_2 is the in-phase component, and the information-carrying X_1PM is the quadrature component of the transmitted signal. After propagating through the channel, the received quadrature signal is passed to the quadrature demodulator, which separates the synchronization X'_2 and information-carrying X'_1PM signals with the use of low-pass filters (LPF). In the QCPSK system, the received information signal $b'(t)$ is detected by first calculating the correlation β between the X'_1PM and Y_1 ($Y_1 \approx X_1$ when synchronized). When detecting "1", X'_1PM positively correlates with Y_1 and $\beta > 0$. When detecting "0", X'_1PM negatively correlates with Y_1 and $\beta < 0$. Then the result of a correlator is processed by a comparator that outputs "1" if $\beta \geq 0$ and "0" if $\beta < 0$, thus acquiring the received information signal $b'(t)$.

The FM-CSK data transmission system in Figure 2 is based on chaos shift keying and frequency modulation. The binary message signal $b(t)$ controls a switch that toggles between chaos signals X_1 and X_3 of equal powers. Bit "1" shifts to X_1, and bit "0" shifts to X_3, thus forming the information-carrying signal X_{13}. The X_2 and X_{13} signals are passed through pre-emphasis filters, and each is used for frequency modulation. Both signals are then transmitted in parallel, propagating through the channel. In the receiver, both signals are passed through a bandpass filter (BPF), frequency-demodulated, and passed through a de-emphasis filter. Using pre-emphasis and de-emphasis filters eliminates noise power spectral density increase with frequency caused by frequency demodulation. The received information signal $b'(t)$ is detected by estimating the correlation between the received X'_{13} signal and Y_1 and Y_3. If X'_{13} correlates with Y_1, then the "1" bit is received, and if X'_{13} correlates with Y_3, then the "0" bit is received. As demonstrated in work [53], an appropriate bit length is selected to minimize the correlation between the modulated bits.

2.2. Vilnius Chaos Oscillator

The chaos oscillator selected for the study of the two systems is the Vilnius chaos oscillator [21]. This oscillator was chosen due to the circuit's simplicity and low power consumption. The circuit diagram of the Vilnius chaos oscillator is given in Figure 3.

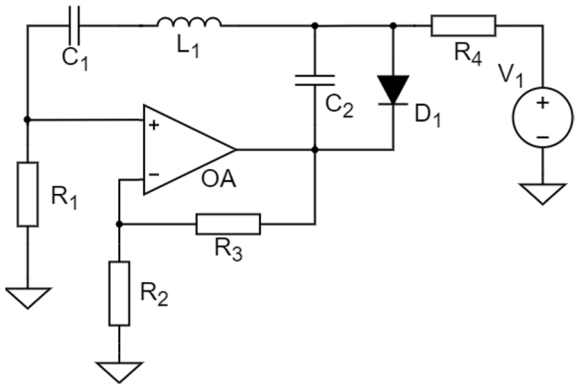

Figure 3. Circuit diagram of Vilnius chaos oscillator.

The mathematical model of the Vilnius chaos oscillator is represented with a set of differential equations:

$$\begin{cases} C_1 \frac{dv_{C_1}}{dt} = i_{L_1}, \\ L_1 \frac{di_{L_1}}{dt} = (k-1)R_1 i_{L_1} - v_{C_1} - v_{C_2}, \\ C_2 \frac{dv_{C_2}}{dt} = i_0 + i_{L_1} - i_D, \end{cases} \quad (1)$$

where v_{C_1} and v_{C_2} are voltages across the capacitors C_1 and C_2; i_{L_1} is the current of the inductor L_1; i_D is the current of the diode D_1; i_0 is the current of the resistor R_4; k is the gain of operational amplifier OA. The given circuit has the following nominals: C_1 = 1 nF; C_2 = 150 pF; L_1 = 1 mH; R_1 = 1 kΩ; R_2 = R_3 = 10 kΩ; R_4 = 20 kΩ; V_1 = 3 V; k = 2. The nonlinear current-voltage characteristic of the diode is given in (2).

$$i_D = i_S \cdot \left(\exp\left(\frac{e v_D}{k_B T} \right) - 1 \right), \quad (2)$$

where i_s is the saturation current; v_D is the saturation voltage; e is the electron charge, k_B is the Boltzmann constant and T is the temperature [21].

The differential equations show that the state variables of the oscillator are the voltages of the capacitors C_1, C_2 and the current of the inductor L_1. The QCPSK and FM-CSK use v_{C_1} and v_{C_2} state variables of the oscillator as X_1 and X_2 (as well as Y_1 and Y_2). In the case of i_{L_1}, the voltage of the R_1 is taken as X_3, knowing that $i_{L_1} = i_{R_3}$. The state variables form a chaotic attractor, and the projections of Vilnius chaos oscillator's attractor are shown in Figure 4a–c.

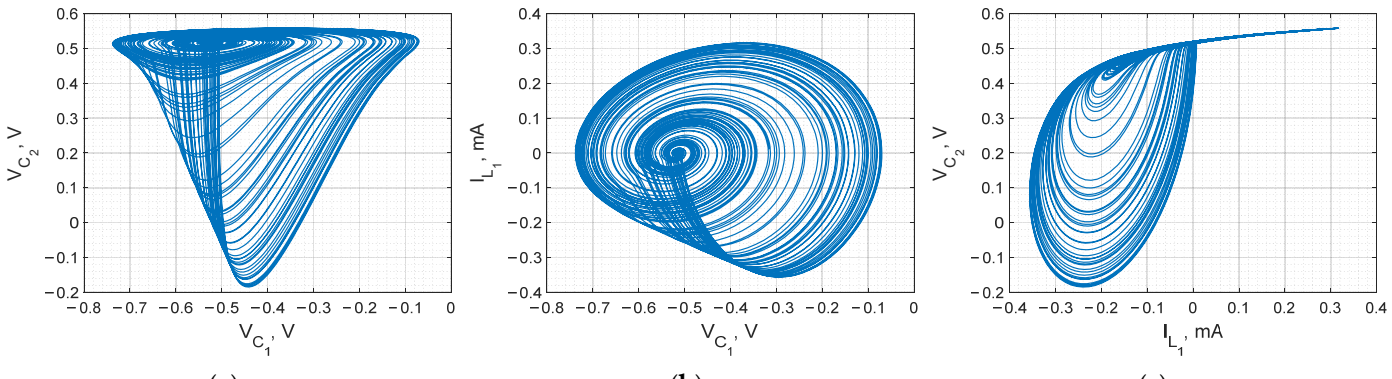

(**a**) (**b**) (**c**)

Figure 4. Vilnius chaos oscillator's attractor projections.

2.3. Hardware Implementation

Figure 5a,b show the block diagrams of the QCPSK and FM-CSK hardware prototypes. The figures demonstrate that the chaos oscillators of the transmitter and receiver, modulators, and demodulators are implemented in hardware for both systems. The information signal generation and detection are done in software on a host computer in MATLAB, while a dedicated Python script provides an interface for controlling the Analog Discovery 2 multifunction oscilloscopes. The device passes the generated information signal $b(t)$ to the transmitter and records the chaos signals used then in MATLAB to detect the message signal $b'(t)$.

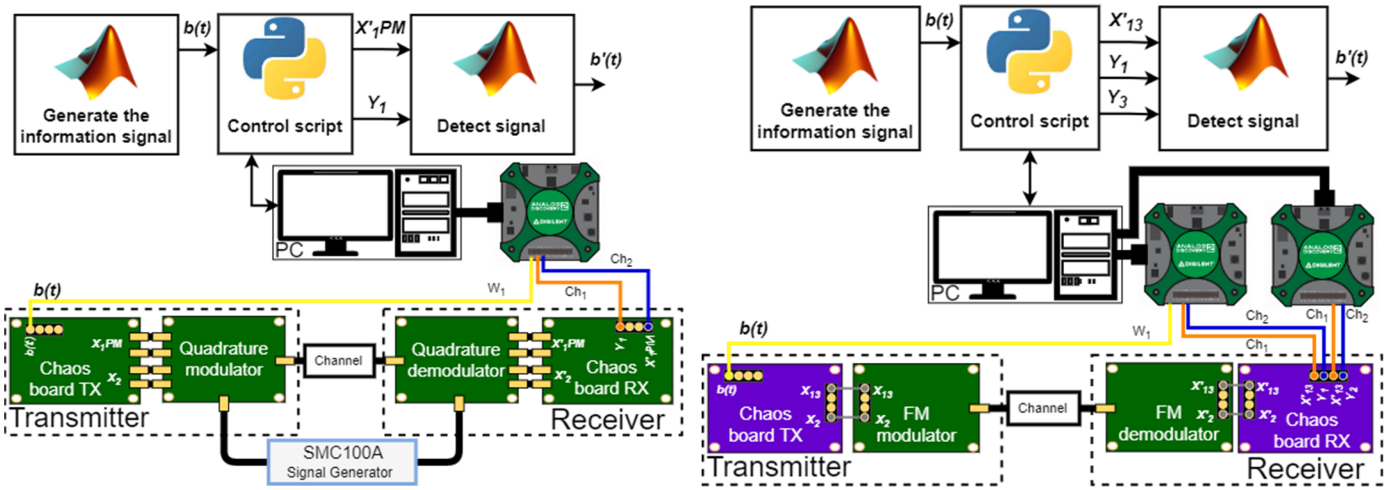

Figure 5. Hardware implementation of the QCPSK (**a**) and FM-CSK (**b**) data transmission system.

The "Chaos board TX" includes a Vilnius chaos oscillator, a chaos shift keying circuit based on DG419 integrated circuit (IC). The board also includes circuitry that pre-processes the chaos signals for the modulators. For the QCPSK system, the quadrature modulator and demodulator are based on AD8346 and AD8347 ICs. The local oscillator signal for the quadrature modulator and demodulator is generated with the Rohde&Schwarz SMC100A signal generator, setting the carrier frequency to 879 MHz. For the FM-CSK system, the FM modulator and demodulator are proprietary FM modules with a 100 MHz carrier frequency. The "Chaos board RX" includes a Vilnius chaos oscillator and the circuitry to post-process the output signals of the demodulators. The works [56,57] elaborate more on the design of the implementation of QCPSK and FM-CSK.

3. Performance in Selective Fading Conditions

A comparative analysis of the QCPSK and FM-CSK systems presented in the previous section aims to evaluate their consistency for usage in WSNs. The mentioned application requires resilience to the phenomena that appear in wireless communications. The principal feature that distinguishes such systems is inter-symbol interference caused by multipath propagation; therefore, this section is mainly devoted to performance analysis in selective fading conditions. A comprehensive description of the test setup is given at the beginning of the section. Since the setup is relevant to the investigation of noise immunity analysis, the performance of the systems in additive white Gaussian noise (AWGN) is also analyzed in this section, which ends with the noise immunity study in selective fading conditions.

3.1. Test Setup

The block diagram of the study is shown in Figure 6. The study uses proposed FM-CSK and QCPSK communication systems, multipath fading simulator, and MATLAB software

for data generation and performance estimation. The general model is similar for both chaos-based communication systems.

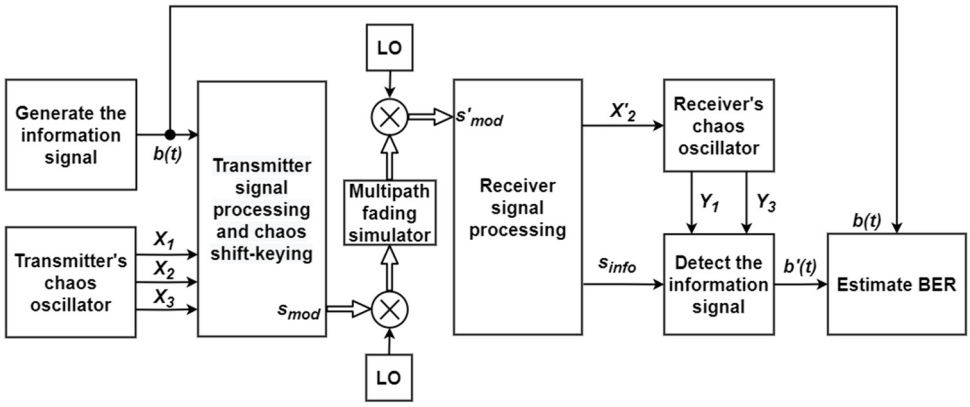

Figure 6. Test setup for the QCPSK and FM-CSK systems' performance estimation in selective fading conditions.

First, the data signal $b(t)$ is created, and the chaos signals of the transmitter's chaos oscillator are acquired. Then the next step applies chaos shift keying using the $b(t)$ and corresponding chaos signals: phase manipulation of X_1 in the case of QCPSK and chaos shift keying between X_1 and X_3 in the case of FM-CSK. The signals are then used for the transmitter signal processing and modulation following their modulation schemes in Figures 1 and 2. The carrier frequency is shifted to the intermediate frequency (IF) of 140 MHz to ensure consistency of the fading simulator input signals for both systems, which is designated by multiplication with the local oscillator (LO) signal in Figure 6. For this study, the two LOs are synchronous, so the carrier recovery is unnecessary in the receiver. The AWGN of the set signal-to-noise ratio (SNR) is applied to the signals before demodulation in the receiver. The received and processed synchronization signal X'_2 is then passed to the receiver's chaos oscillator, and the chaos signals of the oscillator are acquired. The signals are then used to detect the information signal $b'(t)$, following the schemes in Figures 1 and 2. Finally, the bit error rate (BER) is estimated for several SNR levels of the noise signals and different parameters of the noise channel.

The multipath fading simulator is configured to establish two-ray propagation emulation, i.e., the output signal is a weighted sum of the line-of-sight G_{LOS} and reflected G_{MUL} rays. One can easily prove that the model of the emulated channel shown in Figure 7 allows the creation of a notch in the spectra of the transmitted signal.

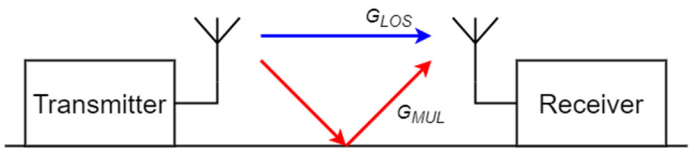

Figure 7. The model of the emulated multipath channel.

For the presented study, the notch frequency equals the IF of 140 MHz. In the number of tests, the depth of the notch differs; however, the system emulates a time-invariant multipath channel, which means that during the operation of a communication system, the configuration of the multipath fading simulator is kept.

The performance of QCPSK and FM-CSK in selective fading conditions is studied in comparison to 4-QAM and FSK systems. The 4-QAM and FSK are the closest non-chaotic counterparts to the studied chaos-based systems, thus providing a good benchmark. Figure 8a,b show the spectra of 4-QAM and QCPSK alongside the estimated amplitude transfer function $|K(f)|$ of the multipath channel. The figure shows that 4-QAM and

QCPSK have the same frequency bandwidth at a –20 dB level. However, in the case of QCPSK, the carrier's amplitude is smaller than the sideband amplitudes, which is not the case in 4-QAM. This difference causes different notches in the spectra of 4-QAM and QCPSK using the same multipath channel parameters. For this reason, the channels' depths are configured differently for 4-QAM and QCPSK but result in the same notch for the two signals at 140 MHz frequency.

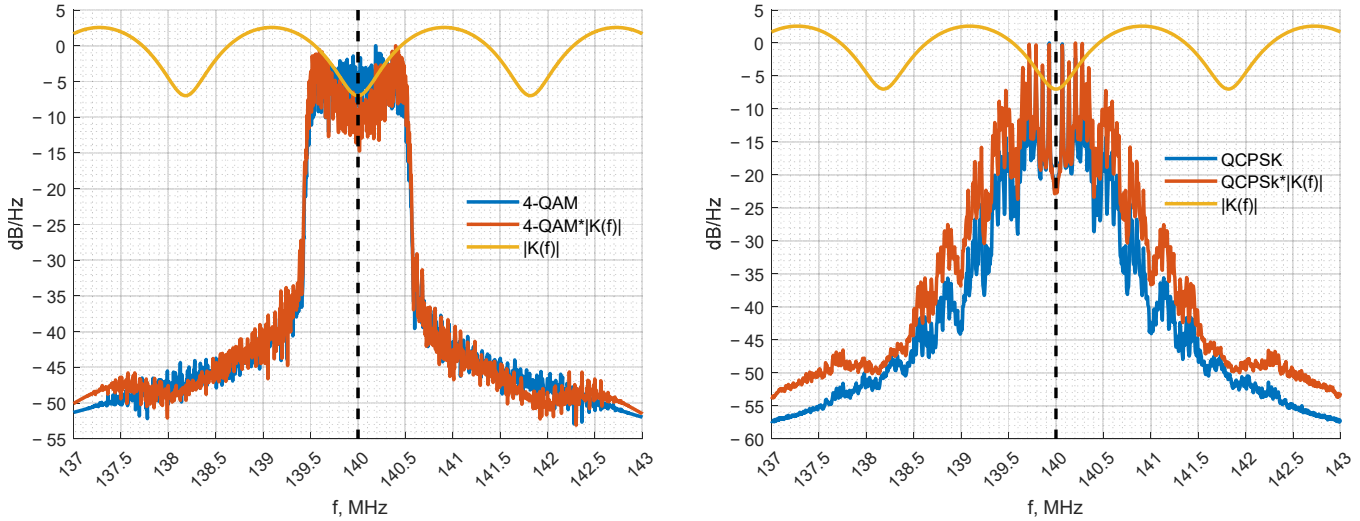

(**a**) (**b**)

Figure 8. The effect of a two-ray channel on 4-QAM (**a**) and QCPSK (**b**).

The FSK system used for the comparison has two carriers that are offset by ±100 kHz from 140 MHz. This configuration makes the FSK's bandwidth match the FM-CSK information-carrying signal's spectra, as seen in Figure 9a,b. The notch frequency for the FSK is set to the lower subcarrier. As in the case of 4-QAM and QCPSK, the channel depths are configured differently yet produce the same depth notch in the signals' spectra.

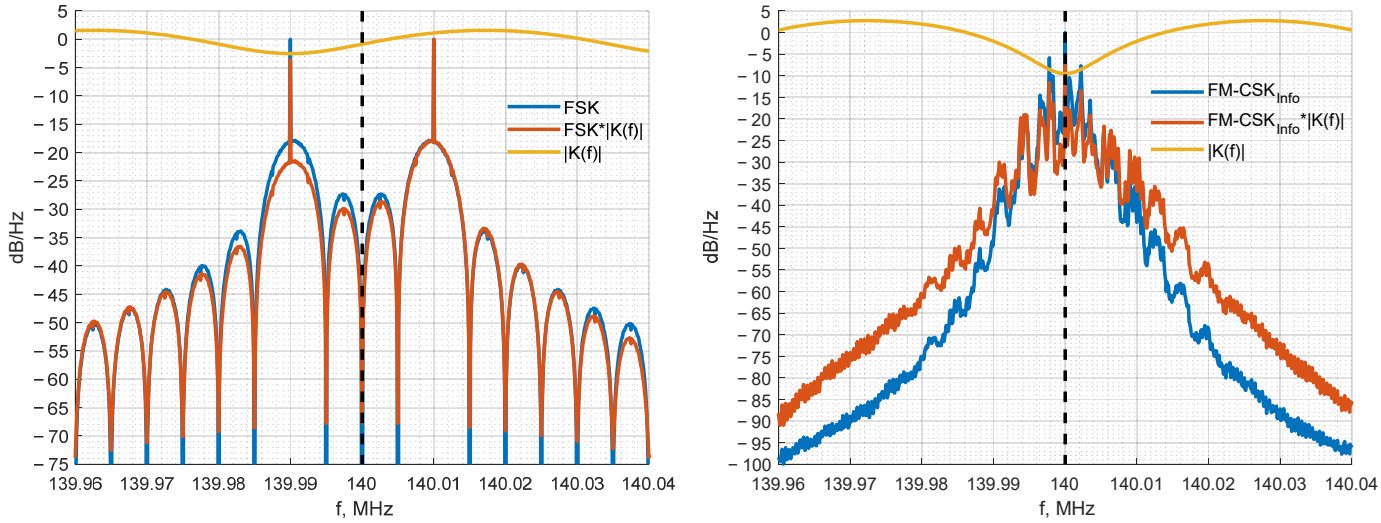

(**a**) (**b**)

Figure 9. The effect of the two-ray propagation on FSK (**a**) and FM-CSK (**b**).

3.2. AWGN Performance Analysis

In the current study, applying attenuation to the demodulated signal controls SNR in the communication system. In the receiver, thermal noise of a constant level is added to the demodulated signal, thus allowing SNR change. The scheme provides an opportunity for sensitivity measurements, yet the SNR stays an implicit parameter. However, the research aims to determine the performance degradation in multipath fading conditions, so it is sufficient to demonstrate relative SNR change. The QCPSK and FM-CSK communication systems' performance in the AWGN channel is presented in Figure 10. For both cases, the received signal level corresponding to BER = 10^{-3} is assumed to be equal to the noise level, i.e., for the AWGN channel, a normalized SNR is 0 dB for this BER level.

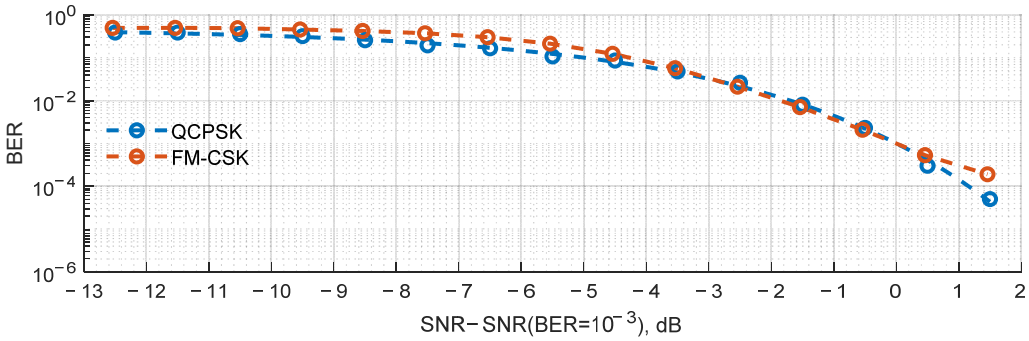

Figure 10. QCPSK and FM-CSK communication systems' performance in the AWGN channel.

For normalized SNR values below −2.7 dB, the QCPSK communication system performs better than the FM-CSK data transmission system. If the normalized SNR is between −2.7 dB and 0 dB, FM-CSK shows almost the same performance in the AWGN channel as the QCPSK system. However, further SNR increase results in better QCPSK communication system performance compared to FM-CSK data transmission system.

3.3. Performance Analysis in the Selective Fading Conditions

The results of the study for the QCPSK and matching 4-QAM systems are presented in Figures 11 and 12. The results for the FM-CSK and FSK systems are presented in Figures 13 and 14. The figures show the SNR influence on BER for several multipath channel spectral notch levels. For the comparability issues and to show the performance degradation dynamics, the SNR is normalized using the approach described for the AWGN channel. Figures 11 and 13 show the approximated curves constructed from the data points.

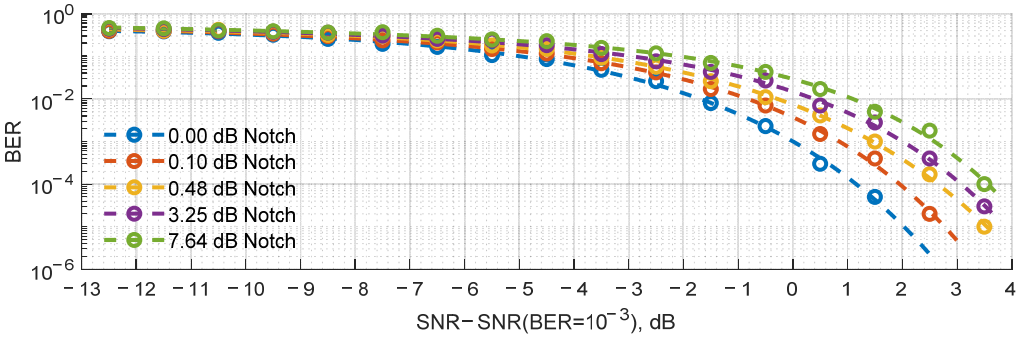

Figure 11. QCPSK communication system's performance for the two-ray channel.

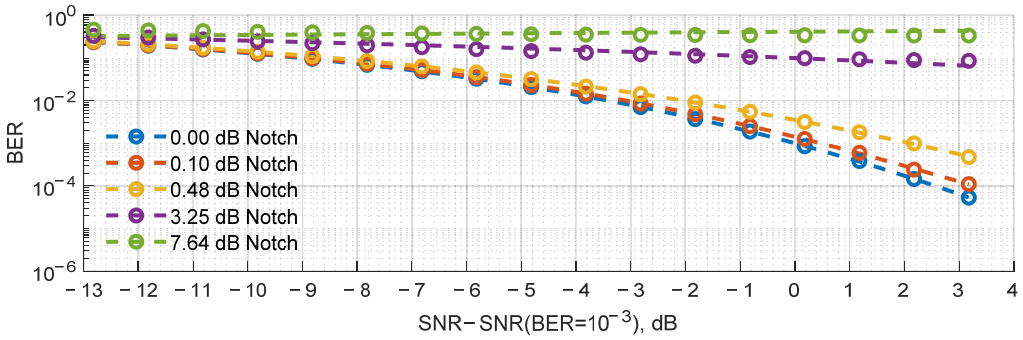

Figure 12. 4-QAM communication system's performance for the two-ray channel.

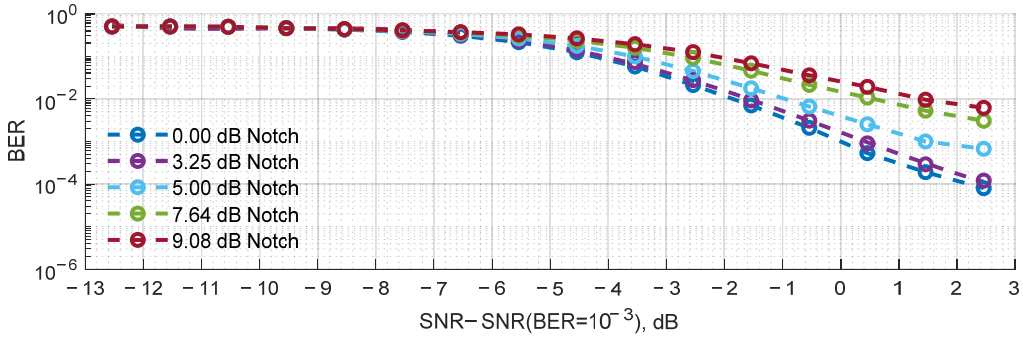

Figure 13. FM-CSK communication system's performance for the two-ray channel.

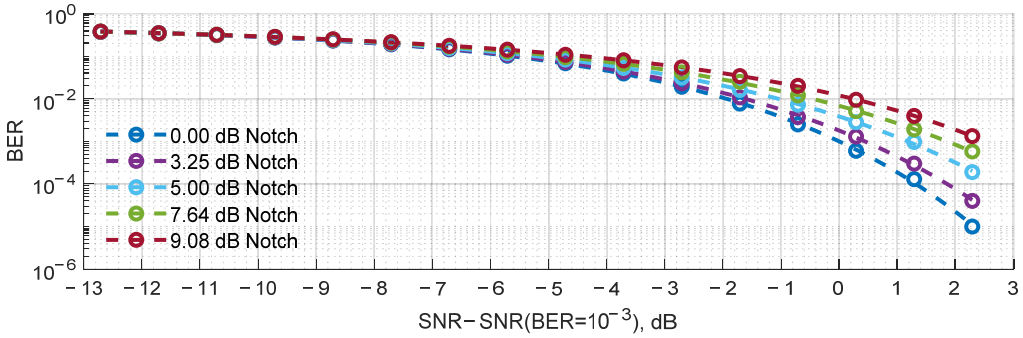

Figure 14. FSK communication system's performance for the two-ray channel.

As one can see in Figures 11–14, SNR is normalized for a 0.00 dB notch at BER = 10^{-3} for all studied communication systems for better side-by-side comparison. QCPSK and 4-QAM data transmission system BER performance (Figures 11 and 12) for a 0.10 dB notch is 3.71 $\times$ 10^{-3} and 1.45 $\times$ 10^{-3}, respectively. Increasing the notch value to 0.48 dB leads to QCPSK communication system BER performance reduction to 7.37 $\times$ 10^{-3}, while BER performance in the 4-QAM data transmission system is 3.42 $\times$ 10^{-3}. A further increase of the notch to 3.25 dB and 7 64 dB significantly reduces the BER performance of the 4-QAM communication system to 9.63 $\times$ 10^{-2} and 3.29 $\times$ 10^{-1}, respectively. At the same notch values, QCPSK data transmission system BER performance is 1.49 $\times$ 10^{-2} and 2.93 $\times$ 10^{-2}, respectively. While at lower notch values (0.10 dB and 0.48 dB) 4-QAM communication system shows better performance, at higher notch values (3.25 dB and 7.64 dB) QCPSK communication system shows significantly better performance.

In the case of FM-CSK and FSK data transmission systems, BER performance (Figures 13 and 14) for a 3.25 dB notch is 1.52 $\times$ 10^{-3} and 1.79 $\times$ 10^{-3}, respectively. For a 5.00 dB notch, both FM-CSK and FSK communication systems, BER performance is similar: 3.92 $\times$ 10^{-3} and 3.83 $\times$ 10^{-3}, respectively. When increasing the notch to 7.64 dB, BER performance is 1.47 $\times$ 10^{-2} and 6.82 $\times$ 10^{-3} for FM-CSK and FSK communication systems.

For the highest investigated notch, 9.08 dB, the BER for FM-CSK and FSK is 2.55×10^{-2} and 1.18×10^{-2} correspondingly. The FM-CSK communication system has a lower BER in the case of a 3.25 dB notch compared to the FSK communication system, while at a 5.00 dB notch the systems performed similarly. However, at notch values 7.64 and 9.08 dB, FSK performs better than FM-CSK.

Comparing communication systems based on chaotic oscillator QCPSK and FM-CSK at a 3.25 dB notch BER is 1.49×10^{-2} and 1.52×10^{-3}, while at a 7.64 dB notch BER is 2.93×10^{-2} and 1.47×10^{-2}. It shows that the FM-CSK communication system for deeper notches performs better than the QCPSK.

4. Performance with Phase Noise

This section is devoted to the QCPSK and FM-CSK systems performance investigation in the increased phase noise conditions. It is applied during the modulation and demodulation processes and is caused by phase deviations in the LO signals. Considering the proportional dependence between the phase noise and the carrier frequency, the current research's relevance to the WSN applications becomes obvious. A typical WSN node uses narrow bandwidth for the transmission; however, the overall number of the nodes tends to increase, which leads to the boost of the carrier frequency and phase noise.

The remaining part of this section describes the test setup and details phase noise generation during the experiments. This section ends with the QCPSK and FM-CSK BER graphs for AWGN conditions at different phase noise levels. The experiments are also performed for the conventional modulation schemes (QPSK and FSK) to show the phase noise immunity benefits of chaos-based systems.

4.1. Test Setup

The general model used for the performance investigation in the presence of phase noise is shown in Figure 5, yet the following modifications have been introduced:

- The multipath fading simulator is replaced by a short connection.
- The LO exploited for the demodulation is modified to introduce adjustable level narrowband noise to the oscillator controlling signal, which yields the following expression for its output signal:

$$s_{LO}(t) = \sin(2\pi f_0 t + \varphi_{noise}), \tag{3}$$

where f_0—frequency of the LO (140 MHz); φ_{noise}—phase noise.

The study assumes the generation of baseband noise with a power spectral density relative to the carrier's power (dBc), which turns to a dual sideband with the same power levels when shifted at the carrier using (3). The measured phase noise of the SMC100 signal generator using an internal oscillator from the datasheet [58] in Figure 15a is used to generate baseband noise with the power spectral density presented in Figure 15b. This approach allows adjusting the levels of the phase noise concerning the actual performance of the generator. While the curves in Figure 15b sweep across frequencies and show different power levels, the power level at 1 Hz is used to adjust the power spectral density level. The value at 1 Hz also refers to the noise curve used for the experiments.

The study investigates the performance of the systems in the AWGN with several power levels of the phase noise signal. This study demonstrates the combined influence of the two noises on the systems' performance.

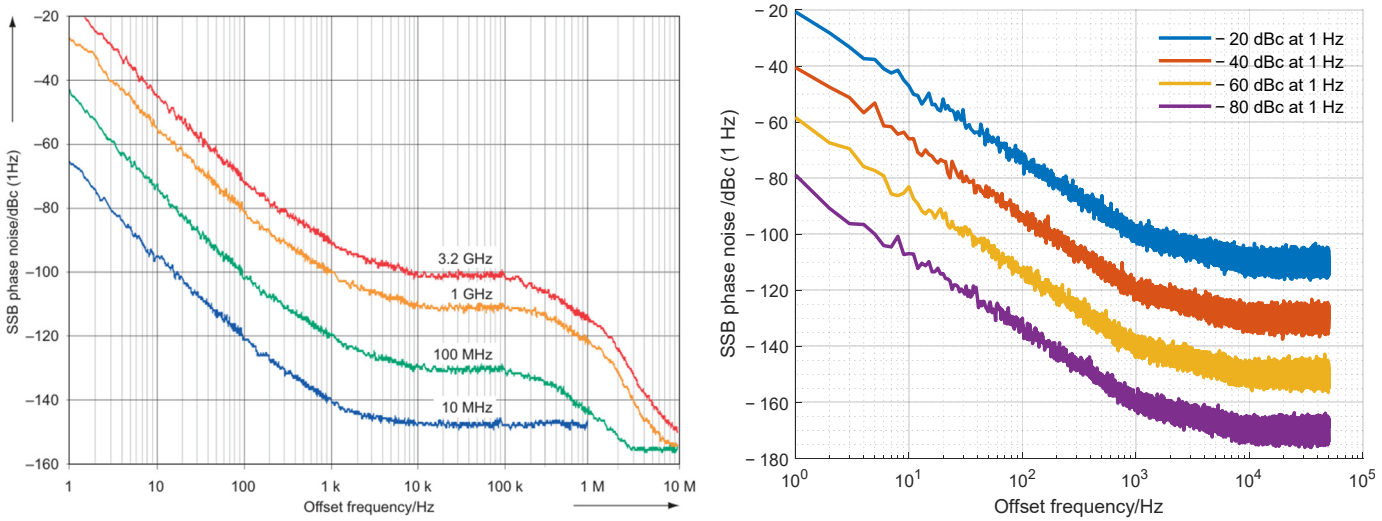

(**a**) (**b**)

Figure 15. SSB phase noise of the SMC100 signal generator [58] (**a**) and generated SSB noise (**b**).

4.2. Result Analysis

The consideration of positive phase noise values reflects the voltage-controlled oscillator (VCO) operation at high frequencies, where the phase noise can be exceptionally high. This is not a typical scenario, yet this study aimed to find the operating limits for each system under phase noise. As was mentioned in the introductory part of the section, an obvious application of these systems fits the requirements of multiple narrowband transmission, such as in WSN or 5G technologies.

The following Figures 16–19 show the results of the second study case, which took several values of the phase noise to analyze the performance of the systems in the AWGN conditions. The SNR levels on the x-axis are normalized to set the 0 dB SNR at the BER = 10^{-3} for comparison issues, like in the selective fading section. The BER curves in Figures 16–19 shows system performance decreasing with the decrease of the SNR. However, at certain phase noise levels, the phase noise influence becomes more dominant, and at higher SNR values, system BER performance does not improve; thus, the BER curves diverge.

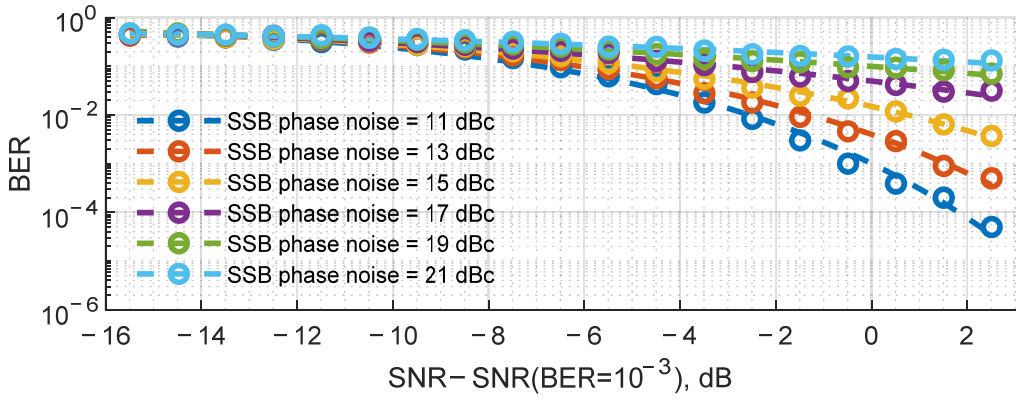

Figure 16. QCPSK system's AWGN performance for several phase noise levels.

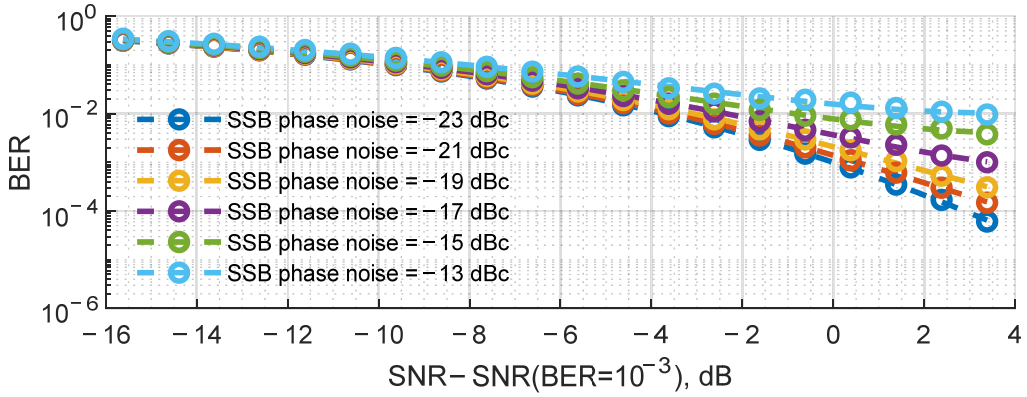

Figure 17. 4-QAM system's AWGN performance for several phase noise levels.

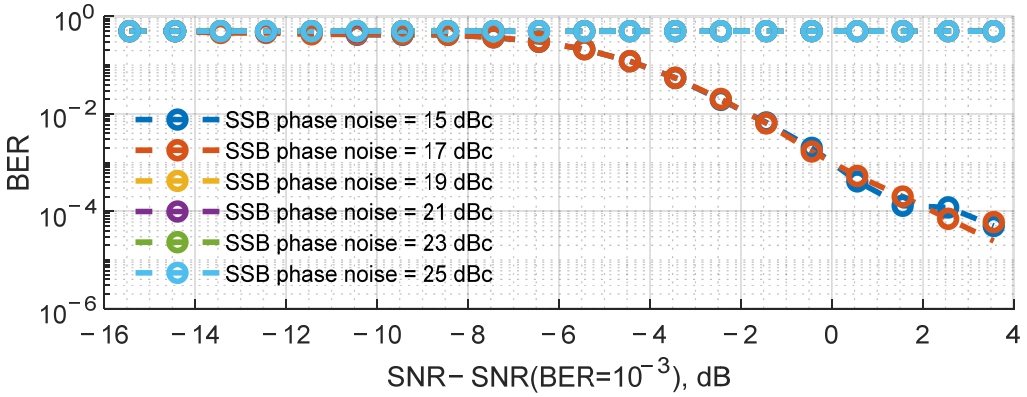

Figure 18. FM-CSK system's AWGN performance for several phase noise levels.

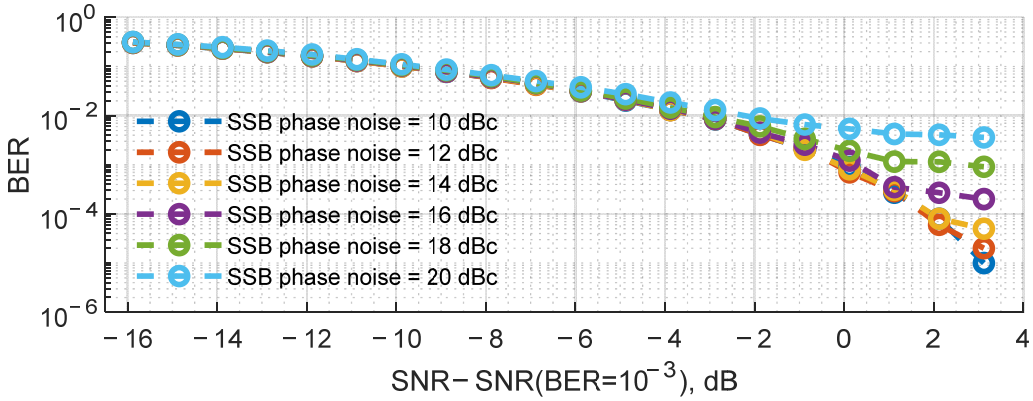

Figure 19. FSK system's AWGN performance for several phase noise levels.

For QCPSK and 4-QAM communication systems (Figures 16 and 17), SNR was normalized at BER 10^{-3}, corresponding to a phase noise of 11 dBc for QCPSK and −23 dBc for 4-QAM. Increasing the phase noise level by 2 dBc, BER performance reduces to 3.98×10^{-3} for QCPSK and 1.48×10^{-3} for 4-QAM. If phase noise grows by an additional 2 dBc, BER performance for QCPSK and 4-QAM is 1.50×10^{-2} and 2.16×10^{-3}, respectively. BER performance for the QCPSK communication system is 4.98×10^{-2}, and 4-QAM performance is 3.91×10^{-3} when an additional 2 dBc of phase noise are added to the communication system. Increasing the phase noise by 2 dBc, QCPSK BER performance is 9.96×10^{-2}, and 4-QAM performance is 8.20×10^{-3}. If the phase noise is increased by 2 dBc, QCPSK and 4-QAM communication systems BER performance is 1.55×10^{-1} and 1.61×10^{-2}, respectively.

For the FM-CSK and FSK communication systems (Figures 18 and 19), SNR was normalized at BER 10^{-3}, corresponding to a phase noise 15 dBc for FM-CSK and 10 dBc for FSK. FM-CSK shows a typical behavior for the systems based on analog frequency modulation [59]. At phase noise levels of 15 dBc and 17 dBc, BER performance is 10^{-3}; however, if the phase noise level increases further, the BER of the system is close to 0.50, meaning the system is useless for data transmission. For the FSK communication system, at phase noise levels of 10 14 dBc, BER performance is 10^{-3}. Increasing the phase noise to 16 dBc BER performance of the FSK is 1.32×10^{-3}. Adding 2 dBc to the phase noise reduces BER performance to 2.01×10^{-3}. At a 20 dBc phase noise, FSK performance is 5.50×10^{-3}.

Comparing QCPSK and FM-CSK communication system performance (Figures 16 and 18) at a phase noise of 15 dBc, QCPSK performance is 1.50×10^{-2}, and FM-CSK performance is 1.00×10^{-3}. If the phase noise is increased to 17 dBc, QCPSK performance is 4.98×10^{-2}, and FM-CSK performance remains unchanged. At phase noise levels higher than 19 dBc, the FM-CSK communication system is useless for data transmission, while the QCPSK communication system is showing better results—at 19 dBc, performance is 9.96×10^{-2}, and at 21 dBc the performance is 1.55×10^{-1}.

4-QAM data transmission system shows a BER decrease with a decrease in phase noise. This is expected behavior, considering both I and Q channels carry information, and cross-interference of the two channels due to phase noise in the mixers degrades the system's performance. The results for FSK are similar, yet this time the performance of the system is affected when the phase noise is in the positive values, meaning that the noise power level is higher than the carrier's power. The results for the QCPSK communication system also show a change in performance with an increase of the phase noise power in the positive values because, similarly to the 4-QAM communication system, the QCPSK system has I and Q channels which are carrying signals. The results for the FM-CSK communication system show a change in performance with an increase of the phase noise power in the positive values. Still, the system's performance changes rapidly when the phase noise level passes a certain threshold, which is typical behavior for systems based on analog FM.

5. Conclusions

The current work aimed to study the use of the Vilnius chaos oscillator in digital communication systems for internet of things (IoT) applications with enhanced physical layer security. Vilnius oscillator was selected due to the circuit's simplicity and low power consumption, thus providing an opportunity for application in wireless sensor networks (WSN) and IoT. The paper analyzed the performance of frequency-modulated chaos shift keying (FM-CSK) and chaos phase-shift keying (QCPSK) in the channel with selective fading and the case of phase noise in comparison with the non-chaotic counterparts of these systems: frequency-shift keying (FSK) and quadrature amplitude modulation (QAM).

The study of selective fading and additive white Gaussian noise (AWGN) impact on the performance of the systems showed that QCPSK demonstrates a lower degradation of BER performance on notch than 4-QAM, while FM-CSK and FSK had a similar degradation dynamic. The analysis of the system's performance limits in the case of phase noise and AWGN demonstrated that the levels of phase noise affecting the performance of the QCPSK are sufficiently higher than that of the 4-QAM. In turn, FSK and FM-CSK showed comparable levels of phase noise which causes performance degradation.

Thus, the results of both studies showed that the dynamic of the performance degradation of chaotic communication systems is more resistant to channels with selective fading or in the case of phase noise, thus demonstrating the advantages of using chaotic waveforms for IoT communication systems in addition to increased physical layer security.

Author Contributions: Formal analysis, R.B., D.C. and F.C.; Funding acquisition, A.L.; Investigation, R.B. and D.C.; Methodology, D.K. and A.L.; Software, R.B. and D.C.; Supervision, D.K. and A.L.; Validation, D.K. and J.G.; Visualization, R.B., D.C., F.C. and J.G.; Writing—original draft, R.B., D.C. and F.C.; Writing—review & editing, F.C., D.K. and A.L. All authors have read and agreed to the published version of the manuscript.

Funding: This work has been supported by the European Social Fund within the Project No 8.2.2.0/20/I/008 «Strengthening of PhD students and academic personnel of Riga Technical University and BA School of Business and Finance in the strategic fields of specialization» of the Specific Objective 8.2.2 «To Strengthen Academic Staff of Higher Education Institutions in Strategic Specialization Areas» of the Operational Program «Growth and Employment». This work has been supported by the Riga Technical University 2021/2022 project for strengthening scientific personnel capacity Nr. ZM-2021/1, "FPGA-based chaotic wireless communication system", Nr. ZM-2021/2, "QCPSK communication system" and Nr. ZM-2021/3, "FM-CSK communication system".

Data Availability Statement: Not applicable.

Conflicts of Interest: The authors declare no conflict of interest.

References

1. Ericsson Mobility Report, November 2022. Available online: https://www.ericsson.com/en/reports-and-papers/mobility-report/reports/november-2022 (accessed on 23 November 2022).
2. Dai, H.-N.; Zheng, Z.; Zhang, Y. Blockchain for Internet of Things: A Survey. *IEEE Internet Things J.* **2019**, *6*, 8076–8094. [CrossRef]
3. Hassija, V.; Chamola, V.; Saxena, V.; Jain, D.; Goyal, P.; Sikdar, B. A Survey on IoT Security: Application Areas, Security Threats, and Solution Architectures. *IEEE Access* **2019**, *7*, 82721–82743. [CrossRef]
4. Frustaci, M.; Pace, P.; Aloi, G.; Fortino, G. Evaluating Critical Security Issues of the IoT World: Present and Future Challenges. *IEEE Internet Things J.* **2018**, *5*, 2483–2495. [CrossRef]
5. Yang, Y.; Wu, L.; Yin, G.; Li, L.; Zhao, H. A Survey on Security and Privacy Issues in Internet-of-Things. *IEEE Internet Things J.* **2017**, *4*, 1250–1258. [CrossRef]
6. Albashier, M.A.M.; Abdaziz, A.; Ghani, H.A. Performance analysis of physical layer security over different error correcting codes in wireless sensor networks. In Proceedings of the 2017 20th International Symposium on Wireless Personal Multimedia Communications (WPMC), Bali, Indonesia, 17–20 December 2017; pp. 191–195.
7. Hamamreh, J.M.; Furqan, H.M.; Arslan, H. Classifications and Applications of Physical Layer Security Techniques for Confidentiality: A Comprehensive Survey. *IEEE Commun. Surv. Tutor.* **2019**, *21*, 1773–1828. [CrossRef]
8. Bendoukha, S.; Abdelmalek, S.; Ouannas, A. Secure communication systems based on the synchronization of chaotic systems. *Stud. Syst. Decis. Control* **2019**, *200*, 281–311. [CrossRef]
9. Stavroulakis, P. *Chaos Applications in Telecommunications*; CRC Press: Boca Raton, FL, USA, 2006; ISBN 978-0-203-02531-4.
10. Wen, H.; Zhang, C.; Chen, P.; Chen, R.; Xu, J.; Liao, Y.; Liang, Z.; Shen, D.; Zhou, L.; Ke, J. A Quantum Chaotic Image Cryptosystem and Its Application in IoT Secure Communication. *IEEE Access* **2021**, *9*, 20481–20492. [CrossRef]
11. Sun, K. *Chaotic Secure Communication: Principles and Technologies*; De Gruyter: Berlin, Germany, 2016; ISBN 978-3-11-043406-4.
12. Rahman, Z.-A.S.A.; Jasim, B.H.; Al-Yasir, Y.I.A.; Abd-Alhameed, R.A. Efficient Colour Image Encryption Algorithm Using a New Fractional-Order Memcapacitive Hyperchaotic System. *Electronics* **2022**, *11*, 1505. [CrossRef]
13. Teodorescu, H.-N. Chaotic Sensors and Tags: Design and Performances. In Proceedings of the 2021 International Conference on Applied Electronics (AE), Pilsen, Czech Republic, 7–8 September 2021; pp. 1–4.
14. Abd, M.H.; Al-Suhail, G.A.; Tahir, F.R.; Ali Ali, A.M.; Abbood, H.A.; Dashtipour, K.; Jamal, S.S.; Ahmad, J. Synchronization of Monostatic Radar Using a Time-Delayed Chaos-Based FM Waveform. *Remote Sens.* **2022**, *14*, 1984. [CrossRef]
15. Zhang, F.; Gao, R.; Huang, Z.; Jiang, C.; Chen, Y.; Zhang, H. Complex Modified Projective Difference Function Synchronization of Coupled Complex Chaotic Systems for Secure Communication in WSNs. *Mathematics* **2022**, *10*, 1202. [CrossRef]
16. Mahmoud, E.E.; Higazy, M.; Al-Harthi, T.M. A new nine-dimensional chaotic lorenz system with quaternion variables: Complicated dynamics, electronic circuit design, anti-anticipating synchronization, and chaotic masking communication application. *Mathematics* **2019**, *7*, 877. [CrossRef]
17. Karimov, T.; Rybin, V.; Kolev, G.; Rodionova, E.; Butusov, D. Chaotic communication system with symmetry-based modulation. *Appl. Sci. Switz.* **2021**, *11*, 3698. [CrossRef]
18. Chua, L.O.; Wu, C.W.; Huang, A.; Zhong, G.Q. A Universal Circuit for Studying and Generating Chaos—Part II: Strange Attractors. *IEEE Trans. Circuits Syst. Fundam. Theory Appl.* **1993**, *40*, 745–761. [CrossRef]
19. Sambas, A.; Mada Sanjaya, W.S.; Mamat, M. Halimatussadiyah Design and analysis bidirectional chaotic synchronization of Rossler circuit and its application for secure communication. *Appl. Math. Sci.* **2013**, *7*, 11–21. [CrossRef]
20. Lorenz, E.N. Deterministic Nonperiodic Flow. *J. Atmospheric Sci.* **1963**, *20*, 130–141. [CrossRef]
21. Tamaševičius, A.; Mykolaitis, G.; Pyragas, V.; Pyragas, K. A simple chaotic oscillator for educational purposes. *Eur. J. Phys.* **2004**, *26*, 61. [CrossRef]

22. Ipatovs, A.; Tjukovs, S.; Pikulins, D.; Grizans, J.; Surmacs, D.; Victor, I.C. Chaos Generation in Hybrid Microcontroller-Based DC-DC Switching Converters. In Proceedings of the 2022 Workshop on Microwave Theory and Techniques in Wireless Communications (MTTW), Riga, Latvia, 5–7 October 2022; pp. 68–71.
23. Pikulin, D. Subharmonic oscillations and chaos in DC-DC switching converters. *Elektron. Ir Elektrotechnika* **2013**, *19*, 33–36. [CrossRef]
24. Pikulin, D. Complete bifurcation analysis of DC-DC converters under current mode control. *J. Phys. Conf. Ser.* **2014**, *482*, 1–9. [CrossRef]
25. May, R.M. Simple mathematical models with very complicated dynamics. *Nature* **1976**, *261*, 459–467. [CrossRef]
26. Russell, D.A.; Hanson, J.D.; Ott, E. Dimension of Strange Attractors. *Phys. Rev. Lett.* **1980**, *45*, 1175–1178. [CrossRef]
27. Hilborn, R.C. *Chaos and Nonlinear Dynamics: An Introduction for Scientists and Engineers*; Oxford University Press: Oxford, UK, 2000; ISBN 978-0-19-850723-9.
28. Butusov, D.; Karimov, A.; Tutueva, A. Hardware-Targeted Semi-Implicit Extrapolation ODE Solvers. In Proceedings of the 2016 International Siberian Conference on Control and Communications (SIBCON), Moscow, Russia, 12–14 May 2016; p. 6.
29. Kaddoum, G. Wireless Chaos-Based Communication Systems: A Comprehensive Survey. *IEEE Access* **2016**, *4*, 2621–2648. [CrossRef]
30. Lee, K.; Kyeong, S.; Kim, J.; Kim, Y.; Park, H. The chaotic on-off keying with guard interval for ultra-wideband communication. In Proceedings of the IEEE VTS Asia Pacific Wireless Communications Symposium, Taipei, Taiwan, 17 February 2006.
31. Kolumban, G.; Kennedy, M.P.; Kis, G.; Jako, Z. FM-DCSK: A novel method for chaotic communications. In Proceedings of the 1998 IEEE International Symposium on Circuits and Systems (ISCAS), Monterey, CA, USA, 31 May–3 June 1998; Volume 4, pp. 477–480.
32. Liu, J.; Wu, Y.X.; Xiao, J.H.; Zhang, Y.H. Chaos-shift-keying secure digital communications using feedback to synchronize Chua's circuit: Simulation and realization. In Proceedings of the International Conference on Communication Technology. ICCT'96, Beijing, China, 5–7 May 1996; Volume 32, pp. 714–715. [CrossRef]
33. Zhu, S.; Xu, Y.; Yin, K. Design of a Quadrature Differential Chaotic Phase Shift Keying Communication System. In Proceedings of the 2009 International Conference on Networks Security, Wireless Communications and Trusted Computing, Wuhan, China, 25–26 April 2009; Volume 1, pp. 518–521.
34. Giurcăneanu, C.D.; Abeywickrama, R.V.; Berber, S. Performance analysis for a chaos-based code-division multiple access system in wide-band channel. *J. Eng.* **2015**, *2015*, 276–284. [CrossRef]
35. Rulkov, N.F.; Sushchik, M.M.; Tsimring, L.S.; Volkovskii, A.R. Digital communication using chaotic-pulse-position modulation. *IEEE Trans. Circuits Syst. Fundam. Theory Appl.* **2001**, *48*, 1436–1444. [CrossRef]
36. Abdullah, H.N. Performance enhancement of FM-QCSK chaotic communication system. In Proceedings of the 2011 3rd International Congress on Ultra Modern Telecommunications and Control Systems and Workshops (ICUMT), Budapest, Hungary, 5–7 October 2011; pp. 1–4.
37. Kaddoum, G.; Roviras, D.; Charg'ey, P.; Fournier-Prunarety, D. Performance of multi-user chaos-based DS-CDMA system over multipath channel. In Proceedings of the 2009 IEEE International Symposium on Circuits and Systems, Taipei, Taiwan, 24–27 May 2009; pp. 2637–2640.
38. Kennedy, M.P.; Kolumban, G.; Kis, G.; Jako, Z. Performance evaluation of FM-DCSK modulation in multipath environments. *IEEE Trans. Circuits Syst. Fundam. Theory Appl.* **2000**, *47*, 1702–1711. [CrossRef]
39. Kuz'min, L.V. Noise immunity of the wireless communications scheme based on ultrawideband chaotic radio pulses in multipath channels. *J. Commun. Technol. Electron.* **2011**, *56*, 367–383. [CrossRef]
40. Babajans, R.; Anstrangs, D.D.; Cirjulina, D.; Aboltins, A.; Litvinenko, A. Noise Immunity of Substitution Method—Based Chaos Synchronization in Vilnius Oscillator. In Proceedings of the 2020 IEEE Microwave Theory and Techniques in Wireless Communications (MTTW), Riga, Latvia, 1–2 October 2020; Volume 1, pp. 237–242.
41. Litvinenko, A.; Aboltins, A. Use of cross-correlation minimization for performance enhancement of chaotic spreading sequence based asynchronous DS-CDMA system. In Proceedings of the 2016 IEEE 4th Workshop on Advances in Information, Electronic and Electrical Engineering (AIEEE), Vilnius, Lithuania, 10–12 November 2016; pp. 1–6.
42. Litvinenko, A.; Beķeris, E. Probability Distribution of Multiple-access Interference in Chaotic Spreading Codes Based on DS-CDMA Communication System. *Electron. Electr. Eng.* **2012**, *123*, 87–90. [CrossRef]
43. Anstrangs, D.D.; Cirjulina, D.; Babajans, R.; Litvinenko, A.; Pikulins, D. Noise Immunity of Chaotic Synchronization in Master-Slave System. In Proceedings of the 2019 IEEE 7th IEEE Workshop on Advances in Information, Electronic and Electrical Engineering (AIEEE), Liepaja, Latvia, 15–16 November 2019. [CrossRef]
44. Kekha Javan, A.A.; Shoeibi, A.; Zare, A.; Hosseini Izadi, N.; Jafari, M.; Alizadehsani, R.; Moridian, P.; Mosavi, A.; Acharya, U.R.; Nahavandi, S. Design of adaptive-robust controller for multi-state synchronization of chaotic systems with unknown and time-varying delays and its application in secure communication. *Sens. Switz.* **2021**, *21*, 254. [CrossRef]
45. Dawa, M.; Herceg, M.; Kaddoum, G. Design and Analysis of Multi-User Faster-Than-Nyquist-DCSK Communication Systems over Multi-Path Fading Channels. *Sensors* **2022**, *22*, 7837. [CrossRef]
46. Meshram, C.; Imoize, A.L.; Elhassouny, A.; Aljaedi, A.; Alharbi, A.R.; Jamal, S.S. IBOOST: A Lightweight Provably Secure Identity-Based Online/Offline Signature Technique Based on FCM for Massive Devices in 5G Wireless Sensor Networks. *IEEE Access* **2021**, *9*, 131336–131347. [CrossRef]

47. Litvinenko, A.; Aboltins, A.; Pikulins, D.; Eidaks, J. Frequency Modulated Chaos Shift Keying System for Wireless Sensor Network. In Proceedings of the 2020 Signal Processing Workshop (SPW), Warsaw, Poland, 5–7 October 2020; pp. 34–39. [CrossRef]
48. Litvinenko, A.; Aboltins, A.; Pikulins, D.; Capligins, F. Chaotic oscillator for LPWAN communication system. In *Chaos and Complex Systems*; Springer: Cham, Switzerland, 2020; pp. 101–115. [CrossRef]
49. Zirem, A.; Senouci, M.R. Efficient lightweight chaotic secure communication system for WSNs and IoT. In Proceedings of the 2018 International Conference on Smart Communications in Network Technologies (SaCoNeT), El Oued, Algeria, 27–31 October 2018; pp. 43–48.
50. Li, B.; Leung, H. A Robust Receiver Based on Chaos Modulation for the Industrial Internet of Things. *IEEE Access* **2021**, *9*, 169309–169320. [CrossRef]
51. Kaddoum, G.; Roviras, D.; Chargé, P.; Fournier-Prunaret, D. Robust synchronization for asynchronous multi-user chaos-based DS-CDMA. *Signal Process.* **2009**, *89*, 807–818. [CrossRef]
52. Hasan, M.Z.; Idris, I.; Uddin, A.F.M.N.; Shahjahan, M. Performance analysis of a coherent chaos-shift keying technique. In Proceedings of the 2012 15th International Conference on Computer and Information Technology (ICCIT), Chittagong, Bangladesh, 22–24 December 2012; pp. 249–254. [CrossRef]
53. Cirjulina, D.; Pikulins, D.; Babajans, R.; Zeltins, M.; Kolosovs, D.; Litvinenko, A. Experimental Study on FM-CSK Communication System for WSN. *Electronics* **2022**, *11*, 1517. [CrossRef]
54. Babajans, R.; Cirjulina, D.; Grizans, J.; Aboltins, A.; Pikulins, D.; Zeltins, M.; Litvinenko, A. Impact of the Chaotic Synchronization's Stability on the Performance of QCPSK Communication System. *Electronics* **2021**, *10*, 640. [CrossRef]
55. Pecora, L.M.; Carroll, T.L. Master stability functions for synchronized coupled systems. *Phys. Rev. Lett.* **1998**, *80*, 2109–2112. [CrossRef]
56. Babajans, R.; Cirjulina, D.; Kolosovs, D.; Litvinenko, A. Quadrature Chaos Phase Shift Keying Communication System Based on Vilnius Chaos Oscillator. In Proceedings of the 2022 Workshop on Microwave Theory and Techniques in Wireless Communications (MTTW), Riga, Latvia, 5–7 October 2022; pp. 5–8. [CrossRef]
57. Cirjulina, D.; Babajans, R.; Kolosovs, D.; Litvinenko, A. Experimental Study on Frequency Modulated Chaos Shift Keying Communication System. In Proceedings of the 2022 Workshop on Microwave Theory and Techniques in Wireless Communications (MTTW), Riga, Latvia, 5–7 October 2022; pp. 1–4. [CrossRef]
58. Rohde & Schwarz SMC100A Signal Generator Specifications. Available online: https://scdn.rohde-schwarz.com/ur/pws/dl_downloads/dl_common_library/dl_brochures_and_datasheets/pdf_1/SMC100A_dat-sw_en.pdf (accessed on 14 October 2022).
59. Rao, P.R. *Analog Communication*; Tata McGraw-Hill Education: New York, NY, USA, 2011; ISBN 978-1-259-08414-0.